Volumetric behavior of some motor and gear-boxes oils at high pressure: compressibility estimation at EHL conditions

María J.G. Guimarey[a], María J.P. Comuñas[a], Enriqueta R. López[a*], Alfredo Amigo[b], Josefa Fernández[a]

[a]Laboratorio de Propiedades Termofísicas, Grupo Nafomat, Departamento de Física Aplicada, Facultad de Física, Universidad de Santiago de Compostela, 15782 Santiago de Compostela, Spain

[b]Laboratorio de Propiedades Termofísicas y Superficiales de Líquidos, Departamento de Física Aplicada, Facultad de Física, Universidad de Santiago de Compostela, 15782 Santiago de Compostela, Spain

Correspondence concerning this article should be addressed to E.R. López at enriqueta.lopez@usc.es

ABSTRACT

Characterization of Elastohydrodynamic Lubrication, EHL, contacts requires an appropriate EoS for the lubricant. Experimental viscosities and speeds of sound of six lubricants from 278.15 to 398.15 K at 0.1 MPa together with densities up to 120 MPa are reported. Tammann-Tait and the two EoSs based on the scaling concept describe the experimental densities of the six oils with average deviations lower to 0.03%. Dowson-Higginson and Zhu and Wen equations currently used in numerical simulations of the EHL regime predict these experimental densities with AADs lower than 0.5%. The prediction ability for volumetric properties, mainly isothermal compressibility, of these five EoSs up to 3000 MPa, which can be reached in EHL lubrication, was evaluated. An asymptotic behaviour is observed when density is plotted versus pressure for Dowson-Higginson and Zhu and Wen equation which is not a realistic behaviour. The EoSs used in the correlations predict more reasonable trends with pressure.

1. INTRODUCTION

Usually liquids are considered incompressible even though their compressibility is an important property that varies with changes in temperature and pressure and cannot be ignored in several situations. For instance, lubricant compressibility is important in many situations as in highly loaded lubricated contacts, such as in ball bearings, gears, and cams and followers, or in most of lubricated metal forming processes.[1] Thus, in several of these contacts the lubrication regime is elastohydrodynamic lubrication (EHL).[2] For instance, two of the three critical tribosystems in automobile engines have full EHL: the cam/follower system and the crank shaft.[3] In the proper lubricant formulation, compressibility and its dependence on pressure must be considered.

At the inlet region of a elastohydrodynamic contact, the relative movement of the surfaces pushes the lubricant into the contact and its viscosity increases exponentially due to the existing high pressures and temperatures.[4, 5] In the central zone (Hertzian region) there is a sufficient amount of lubricant to separate both surfaces, known as central film thickness.[4] The increase in viscosity causes the lubricant to be in a pseudoplastic state. In the outlet region the lubricant undergoes a marked decrease in pressure and therefore in viscosity. This decrease in viscosity at values close to ambient pressure causes a narrowing of the film thickness so as to maintain constant lubricant flow. The thickness in this area is known as the minimum film thickness. The decrease in film thickness causes a pressure peak which depends on the pressure-viscosity characteristics of the lubricant.[4]

An appropriate equation of state (EoS) for the lubricant is necessary to obtain representative predictions of practical properties of EHL contacts. It was proven that for most practical load conditions, the central film thickness is quite significantly reduced due to the compressibility, although the effect on the minimum film thickness is lower.[6, 7] Thus, lubricants with high compressibility give a thinner central film than a stiffer lubricant for the same inlet

oil film thickness.[8] The effect of the density-pressure relation on other EHL parameters such as pressure spikes has been also studied by several authors[7, 9] finding that an incompressible lubricant gives rise to much higher pressure at the pressure spike than compressible oils.

In addition, from both the fundamental and practical points of view, the knowledge at elevated pressures of thermophysical properties of fluids is crucial to verify current and to develop new reliable EoS, which are needed in several chemical engineering areas as to design new processes and plants or to optimize the existing ones.

In this work we report the isothermal compressibilities, κ_T, up to 100 MPa in the temperature range from 278.15 K to 398.15 K of four base lubricants and two formulated lubricants. The isothermal compressibilities have been obtained from new high pressure density values measured at pressures up to 120 MPa in the same temperature range. In addition, the six lubricants have been characterized in terms of density, viscosity, speed of sound and adiabatic compressibility at atmospheric pressure. Adiabatic compressibility can be used to predict the pressure-viscosity coefficient of lubricants.[10] Thus Mia[11] proposed exponential empirical correlations between both properties and introduce the sound velocity as a predicting parameter for tribological properties and lubricant rheology. The correlation ability of three different EoS for fitting experimental density values as a function of temperature and pressure was checked. The first one is the Tammann-Tait equation and the other two are the Power-Law Density Scaling (PLDS)[12, 13] and the General Density Scaling (GDS)[13, 14] EoSs. Additionally, the density predictive capability of three EoS, currently used in numerical simulations of EHL lubrication was also analyzed for the studied lubricants. These EoS are those from Dowson-Higginson[15, 16], Zhu and Wen[17] and Jacobson-Vinet.[18] Isothermal compressibilities have been calculated from the five first equations, in order to check their capability to extrapolate data up to 3 GPa, which can be reached in EHL contacts.

2. EXPERIMENTAL

2.1. Materials. Samples of six lubricants have been provided by REPSOL. The lubricants are four bases of the Group I (saturates < 90% and/or sulfur > 0.03%, viscosity index between 80 and 120), Group III (saturates > 90%, sulfur < 0.03%, viscosity index ≥120), Group IV (a polyalphaolefin, PAO6) and Group V (a mixture of unsaturated esters of trimethylolpropane and of neopentylglycol) and two formulated lubricants: a gear oil and a motor oil. The gear oil contains polyalkyl methacrylate, PAMA, as additive to improve the viscosity index. Table 1 reports their density and dynamic viscosity at 313.15 K together with the viscosity index measured in this work with a Stabinger viscometer.

Table 1. Properties of the fluids studied in this work.

Fluids	Sample	ρ(kg·m^{-3}) at 313.15 K*	η(mPa·s) at 313.15 K*	VI*
Base oil G-I	SN-230	866.7	41.8	98
Base oil G-III	6 cSt	826.1	30.1	129
Base oil G-IV	PAO-6	811.1	24.1	137
Base oil G-V	Ester	902.4	34.8	191
Gear oil	75 W 90	863.7	56.6	228
Motor oil	15 W 40	873.3	91.0	138

*Determined in this work with Stabinger viscometer SVM3000**.** Expanded uncertainties (k=2): $U(T)$ is 0.02 K from 288.15 K to 378.15 K and 0.05 K outside this range; $U(\rho)$= 0.5 kg·m^{-3}; $U(\eta)$=1%

2.2. Measurement techniques. Densities and viscosities at atmospheric pressure have been measured between 278.15 and 373.15 K with an automated SVM 3000 Anton Paar rotational Stabinger device,[19] which includes a vibrating tube densimeter. A further description of our device can be found in literature.[20, 21] This apparatus provides also the viscosity index (VI). The SVM 3000 uses Peltier elements for fast and efficient thermostating. The temperature uncertainty is 0.02 K from 288.15 K to

378.15 K and 0.05 K outside this range. The uncertainty of the dynamic viscosity is 1% whereas density is measured with an expanded uncertainty[21, 22] of 0.5 kg·m^{-3}.

Densities at atmospheric pressure in the temperature range 283.15 to 338.15 K were also determined with an Anton Paar DSA 5000 which allows to measure density with an expanded uncertainty (k=2) of 0.01 kg·m^{-3}. This apparatus is equipped with another cell to measure also the speed of sound, with an expanded uncertainty (k=2) of 1 m·s^{-1}. The temperature is kept constant within ±0.005 K.

Density measurements up to 120 MPa, in the temperature range from 278.15 K to 398.15 K, were performed in a vibrating tube densimeter Anton Paar HPM.[23-28] This equipment, fully automated except the operations of filling and cleaning, has previously described in detail.[23] The heart of the setup is an Anton Paar HPM vibrating tube densimeter. The temperature of the vibrating tube cell is measured with a Pt100 thermometer with an uncertainty of 0.02 K. The pressure of the system was measured by using a HBM Digibar II K-PE3000 pressure transducer, being 0.02 MPa the uncertainty. The densimeter was calibrated with vacuum, water[29] and n-decane[30, 31] following the procedure proposed by Comuñas *et al.*[32] Taking into account the uncertainties of the temperature, pressure, water and decane density and oscillation period measurements for water, decane, vacuum and the studied liquid, it was estimated[23] that the expanded (k=2) density uncertainty is 0.7 kg·m^{-3} for temperatures below T = 373.15 K, 5 kg·m^{-3} at T = (373.15 and 398.15) K and p = 0.1 MPa, and 3 kg·m^{-3} at $T \geq 373.15$ K and p > 0.1 MPa. Reliability of the apparatus and its calibration were tested by measuring density of n-decane. Absolute average deviation (AAD%) of 0.07% and 0.05% were obtained between the experimental density data and values reported by Cibulka and Hnedkovsky[31] and by Lemmon and Span[29] respectively.

3. RESULTS AND DISCUSSION

3.1. Densities, viscosity and speed of sound at 0.1 MPa. The densities at atmospheric pressure measured with the Stabinger and DSA 5000 densimeters are reported in Tables S1 and S2 respectively. Deviations between the results obtained with both apparatuses are lower than 0.08%, which is in agreement with the combined uncertainties of both setups.

In Figure 1 we have plotted the experimental densities measured with the Stabinger densimeter. As can be seen G-V is the denser fluid of the four base oils whereas PAO6 has the lower density. This is due to the ester groups of G-V which increase the packing of the molecules because of their attractive dipole intermolecular forces whereas PAO6 is apolar and contains only single C-H bonds. The density of the G-III oil is lower than that of the G-I oil due to the former contains more saturated compounds, i.e., lower intermolecular forces. Concerning formulated oils, a difference of 1% is observed between gear and motor oils densities over the entire temperature interval at 0.1 MPa.

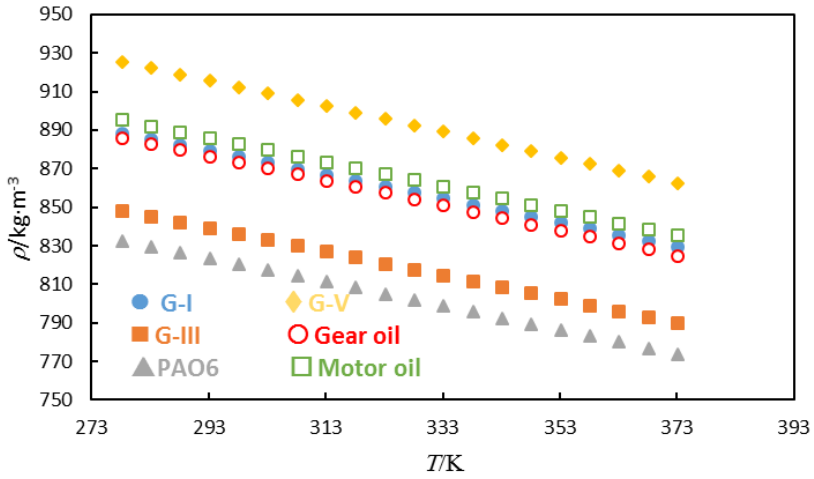

Figure 1. Densities at 0.1 MPa measured with the Stabinger densimeter for the six oils studied.

The speeds of sound in the six oils are presented in Table S2. As can be observed this property presents the highest values for G-I and the lowest for PAO6. For the formulated oils we found the highest values for the motor oil. The variation of the speed of sound over the entire temperature range is around 14% for the six oils.

Isentropic compressibility, κ_S, was determined from the density and speed of sound measurements by means of Laplace equation:

$$\kappa_S = \frac{1}{\rho u^2} \quad (1)$$

The trend obtained for this property (Figure 2) is PAO6 > G-III > gear oil > motor oil ≈ G-I > G-V. The high compressibility of the PAO6 is due to its slight intermolecular forces and the flexibility of their molecules whereas molecules of the complex ester of G-V are more strongly associated. The inverse of the isentropic compressibility is the adiabatic bulk modulus. Both adiabatic bulk modulus and the viscoelastic solid transition temperature depend on the samples bulk property. Mia and Ohno[33] have found that lubricating oils of low adiabatic bulk modulus present a better fluidity at low temperatures. Consequently, it is expected that the better low-temperature behavior corresponds to PAO6 and the poorest to G-V.

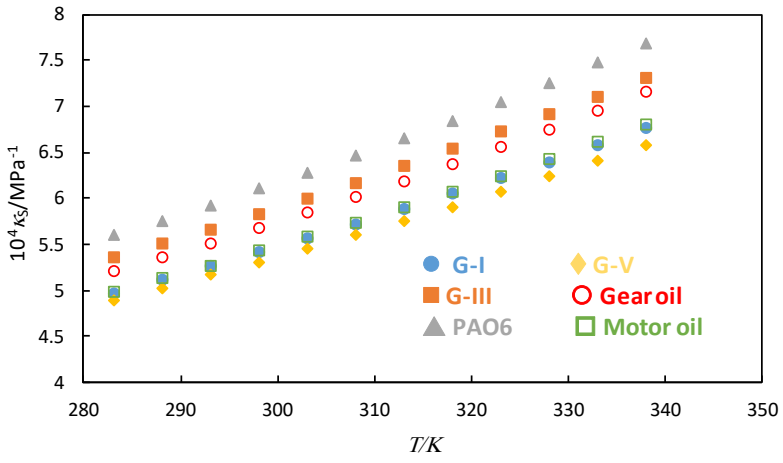

Figure 2. Isentropic compressibilities at 0.1 MPa for the six oils studied.

Dynamic viscosities are reported in Table S1 and plotted versus temperature in Figure 3. As can be observed at the lowest temperatures the most viscous oil is the motor oil (812.7 mPa·s at 278.15 K). The behavior of the viscosity at 0.1 MPa as a function of temperature, $\eta(T)$, was described using the following modification of Andrade's equation also known as three-coefficient Vogel-Fulcher-Tammann (VFT) equation:

$$\eta = A\exp\left(\frac{B}{T-C}\right) \qquad (2)$$

The values obtained for *A*, *B* and *C* are gathered in Table S3. The average absolute deviations,[34] AAD, of these correlations are lower than 1.3% for all the base oils. The glass-transition temperature is often defined as that at which the shear viscosity of the liquid is 10^{12} Pa·s.[35] Following this definition, we have estimated the T_g values from eq 2 with the parameters indicated in Table S3 by extrapolating the viscosity to that value. The obtained values are 190 K, 181 K, 172 K, 177 K, 188 K and 183 K for G-I, G-III, PAO6, G-V, motor oil and gear oil respectively. Different authors have found that the resulting temperature using this definition and VFT can differ from the glass transition temperature obtained from DSC measurements for glass-forming liquids up to 25 K.[36-38] Nevertheless, it has been found that the viscosity of squalane at T_g should be lower than the universal value of 10^{12} Pa·s.[39]

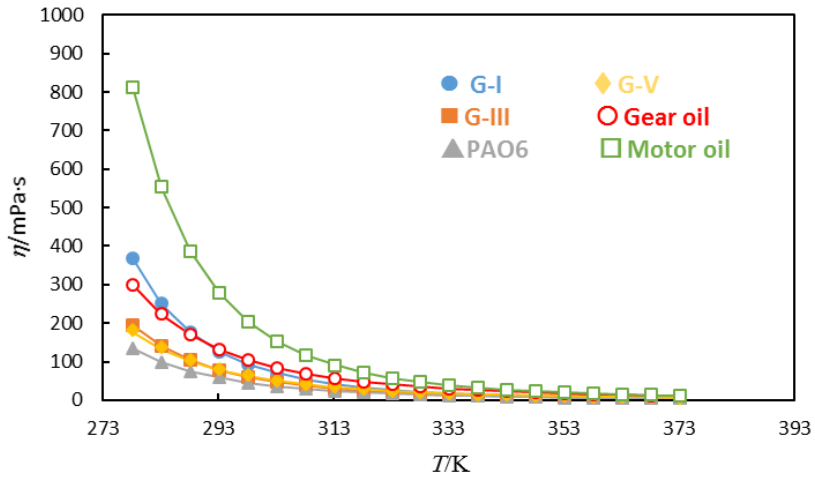

Figure 3. Dynamic viscosities measured at 0.1 MPa for the six oils studied. Solid lines represent the VFT correlations (eq 2 with parameters reported in Table S1)

3.2. Densities at high pressures. The experimental density values measured with the HPM densimeter up to 120 MPa are presented in Table S4. As an example, the variation of the density with temperature and with pressure for PAO6 and G-V, respectively, is presented in Figure 4.

The increase of the density with pressure is similar for the six oils, thus an average increase around 5% is observed at the lower temperature (278.15 K) and around 8% at the higher temperature (398.15 K).

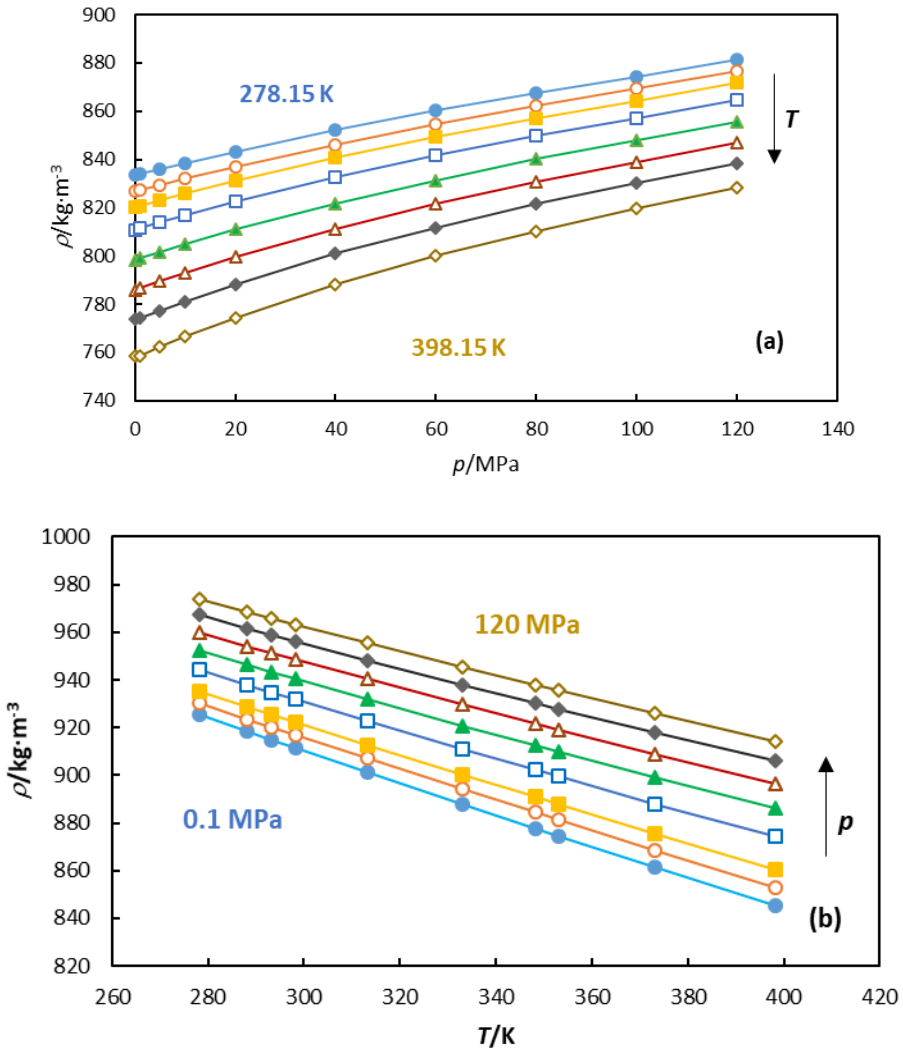

Figure 4. Experimental densities measured with the HPM densimeter from 0.1 MPa up to 120 MPa. (a) PAO6: ● 278.15 K, ○ 288.15 K, ■ 298.15 K, □ 313.15 K, ▲ 333.15 K, △ 353.15 K, ◆ 373.15 K, ◇ 398.15 K and (b) G-V: ● 0.1 MPa, ○ 10 MPa, ■ 20 MPa, □ 40 MPa, ▲ 60 MPa, △ 80 MPa, ◆ 100 MPa, ◇ 120 MPa

To correlate the experimental values, we have used three EoS. One of them is the modified Tammann-Tait equation:

$$\rho(T,p)=\frac{\rho(T,p_0)}{1-C\ln\left(\frac{B(T)+p}{B(T)+p_0}\right)} \tag{3}$$

where $\rho(T,p_0)$ is the temperature dependence of the fluid density at the reference pressure p_0= 0.1 MPa. Polynomial functions of temperature were used for $\rho(T,p_0)$ and $B(T)$:

$$\rho(T,p_0)=A_0+A_1T+A_2T^2 \tag{4}$$

and

$$B(T)=B_0+B_1T+B_2T^2 \tag{5}$$

The other two equations used to correlate density values for the six oils are due to Grzybowski *et al.*[12-14] The first one, the Power-Law Density Scaling EoS (PLDS),[12] has the following expression:

$$V(T,p)=\frac{V(T,p_0)}{\left[1+\frac{\gamma_{EOS}(p-p_0)}{B_T(p_0)}\right]^{1/\gamma_{EOS}}} \tag{6}$$

with

$$V(T,p_0)=V_0=\frac{1}{\rho(T,p_0)}=A_0+A_1(T-T_0)+A_2(T-T_0)^2+A_3(T-T_0)^3 \tag{7}$$

and

$$B_T(p_0)=b_0\exp[-b_2(T-T_0)] \tag{8}$$

where the subscript 0 refers to an arbitrarily chosen reference state. A_i, b_j and the scaling exponent γ_{EOS} are adjustable parameters. In this work 0.1 MPa was chosen as a reference pressure, p_0, whereas for T_0 we have used 278.15 K. The second equation proposed by Grzybowski *et al.*, General Density Scaling EoS (GDS),[14] takes the form:

$$V(T,p)=\exp\left(\frac{C_1-\left(C_1^2+4C_2^2\ln^2V_0-4C_2C_1\ln V_0+4C_2\ln\left[1+\frac{\gamma(V_0)(p-p_0)}{B_T(p_0)}\right]\right)^{1/2}}{2C_2}\right) \tag{9}$$

being

$$\gamma(V_0) = C_1 - 2C_2 \ln V_0 \quad (10)$$

and where $V(T,p_0)=V_0$ is given by eq 7 and $B_T(p_0)$ by eq 8.

The set of fitting coefficient values (A_i, for eq 7, b_i and γ_{EOS} for eq 6 and b_i, and C_i for eq 9) together with the standard deviations, σ for the values at atmospheric pressure and σ^* for the fits of the data at pressures different to the atmospheric one are listed in Tables S5 and S6. The standard deviations are lower than the experimental uncertainty for the six oils. The three equations correlate the experimental data excellently, with average absolute deviations[34] AADs, lower or equal to 0.03%. The lowest-quality fit corresponds to motor oil with Tammann-Tait equation for which the maximum deviation (0.14%) was found.

The experimental values reported in this work offer an opportunity to test the predictive capability of three equations usually used in EHL simulation. The first equation that we have used is known as Dowson-Higginson (DH) EoS[15, 16]:[15, 16]

$$\rho(T, p) = \rho(T, 0.1)\left(1 + \frac{0.6p}{1+1.7p}\right) \quad (11)$$

where $\rho(T,0.1)$ is given by eq 4, T is the temperature in K and p is the pressure in GPa. This expression was obtained by Dowson *et al.*[16] fitting isothermal data of a mineral oil up to 350 MPa, but it is used as universal EoS in EHL lubrication. The second one, due to Zhu and Wen[17] (ZW EoS), introduce in eq 11 an explicit temperature dependence:

$$\rho(T, p) = \rho(T_0, 0.1)\left(1 + \frac{0.6p}{1+1.7p} - 0.65\cdot10^{-3}(T - T_0)\right) \quad (12)$$

where T is the temperature in K, p is the pressure in GPa and T_0 is a reference temperature. Similarly to PLDS and GDS EoSs, for eq 12 we have chosen T_0=278.15 K. When $T=T_o$, eq 12 reduces to eq 11. Finally the third relation is that proposed by Jacobson-Vinet[18] (JV EoS):

$$p = 3B_0\left(\frac{\rho_0}{\rho}\right)^{-2/3}\left[1-\left(\frac{\rho_0}{\rho}\right)^{1/3}\right]\exp\left[\eta'\left[1-\left(\frac{\rho_0}{\rho}\right)^{1/3}\right]\right] \quad (13)$$

where B_0 and η' are temperature-independent characteristic parameters and ρ_0 is the experimental density at 0.1 MPa for the corresponding isotherm. Venner and Bos[6] used this equation in numerical EHL simulations of an isothermal contact with a mineral oil considering that B_0=1.7·10^{-9} Pa and η'=10.0.

Remarkable agreement between the experimental and predicted densities was found for eqs 11 and 12. DH EoS predicts the density values of the six oils with AADs[34] ranging from 0.34% for G-V up to 0.50% for PAO6. The densities predicted from the ZW EoS[17] present even lower deviations with the experimental values (an AAD lower or equal to 0.34% was found for the six oils). In terms of pressure, with eq 13, AADs ranging from 21% for G-V up to 33% for PAO6 (0.44% and 0.74% in terms of densities, being the corresponding bias 0.36% and 0.73%) were obtained. Hence, JV EoS predicts slightly worse than DH and ZW EoSs. In general, predicted densities are greater than the experimental ones. Additionally, this equation is slightly inconvenient for their use as EHL EoS because it cannot be easily inverted analytically[6]. The poorest predictions of the JV equation[18] and of Dowson and Higginson could be explained by the fact that both empirical equations are based on considering that the bulk modulus (the inverse of the isothermal compressibility) is temperature independent, which is not the case for the six oils studied in this work (Tables S4-S6). Similar results have been found previously.[40]

DH and ZW EoSs are employed to estimate film thicknesses in EHL. In this lubrication regime the range of conditions is quite broad and can reach pressures up to 500-3000 MPa.[41] The temperature is dependent of the gearbox characteristics and of the lubricant properties.[42] The typical operating temperatures for the gear flank and bearing ring and roller are around 343.15-353.15 K[42, 43].[42, 43] With the aim to check the ability of the three correlation EoSs (Tammann-Tait, PLDS and GDS) to extrapolate density values as well as the predictive

capability of DH[15] and ZW[17] equations, we have chosen another oil (Santotrac 100 (SN100)) for which density values have been measured by Ohno *et al.*[44, 45] over a broad pressure interval (0.1-1146) MPa and from 313 to 353 K. These authors[44] indicated that SN100 changes to amorphous solid state at high pressures and lower temperatures. For the purpose to analyze the extrapolation capability of the EoSs, we have correlated with eqs 3, 6 and 9 the experimental density values of Ohno *et al.* up to 200 MPa and after that we extrapolate up to 1100 MPa. For eqs 7 and 12 we have used T_0=313 K, which is the lowest temperature of the experimental densities for this oil.

In Figure 5 we plot the experimental[44, 45] and predicted densities using the five equations for SN100 at 313, 333 and 353 K. For Tammann-Tait, PLDS and GDS EoSs the densities up to 200 MPa are correlated values. As can be observed at 313 K (Figure 5a) the best prediction results correspond to those provided by both predictive equations (at the reference temperature T_0=313 K the predicted values obtained with both equations are identical) whereas when temperature increases these EoSs are inadequate even at the lower pressures to predict the density values. The good results of both prediction equations at 313 K are due to the behavior of the isothermal compressibility, which become very low and constant[44] (elastic-plastic transition) at lower pressures than at the higher 353 K.

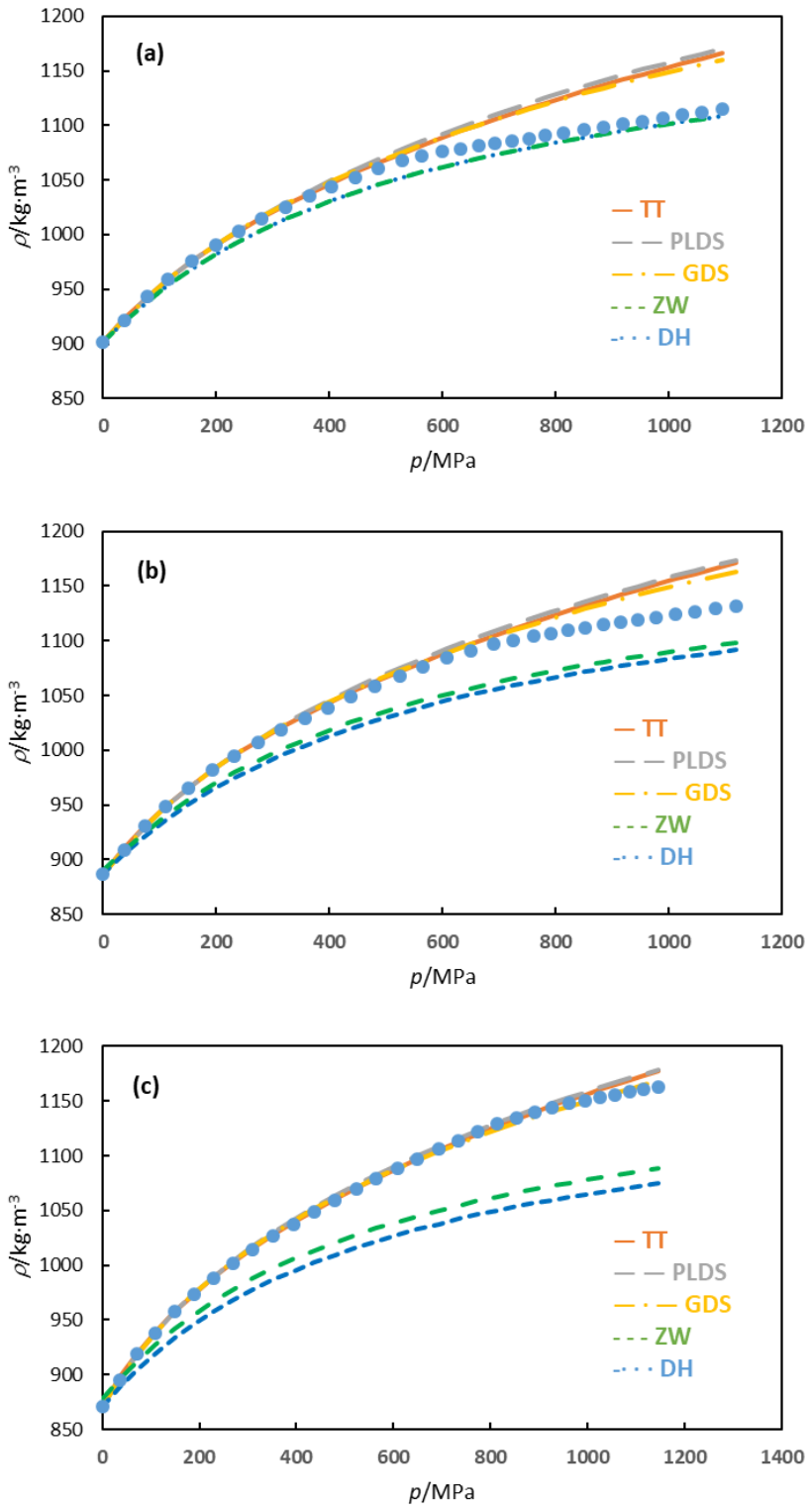

Figure 5. Density pressure behavior of SN100 at (a) 313 K, (b) 333 K and (c) 353 K. Experimental densities reported by Ohno *et al.*[44, 45] (●). For Tammann-Tait, PLDS and GDS EoSs (eqs 3, 6 and 9, respectively) lines represent correlated values up to 200 MPa and predicted

densities up to 1100 MPa whereas for DH (eq 11) and ZW (eq 12) EoS the entire isotherms are predicted values.

For the higher temperatures,[44] DH EoS predicts worse that ZW EoS because its isothermal compressibility is temperature independent contrarily to the experimental values.[40] In addition the capability of both predictive equations (DH and ZW) to estimate densities at the highest temperature is also inappropriate because, as expected, an asymptotic behavior is predicted as pressure increases, which is not, in general, a realistic behavior for this property.[6, 40, 46] Thus, the best predictions at the higher temperatures are those delivered by the GDS EoS (AAD%=0.92%). Nevertheless, we must point out that none of the correlating equations, with the parameters obtained fitting the data up to 200 MPa, are able to reproduce the temperature behavior of the experimental densities at high pressures because the experimental density dependence is stronger than that predicted by these three EoSs. This fact can be seen in Figure S1(a) of the supplementary information where the results obtained with the GDS EoS are plotted together with the experimental densities.

Besides, we have fitted all the experimental density values of the SN100 oil. Figure S1(b) of the supplementary information shows that GDS EoS describes well the density behavior up to a pressure around 400 MPa. Nevertheless, at higher pressures the predicted isothermal curves are much closer to each other than the experimental ones. From our point of view the $p\rho T$ behavior of this oil is very difficult to describe due the abrupt changes of the bulk modulus-pressure curves caused by the oil solidification.[44] Similar results are obtained with the Tait and PLDS EoS.

Using the Tammann-Tait, PLDS and GDS EoSs correlations as well as the prediction methods given by eqs 11 and 12, we have predicted the density values up to 3000 MPa for the six oils analyzed in this work. Note that for the three correlation EoSs the prediction is performed only for pressures higher than 120 MPa and up to 3000 MPa. In Figure 6 we have

plotted the results for G-V at the different experimental temperatures. As can be observed at temperatures up to 313 K both predictive methods give density values higher than the experimental ones at pressures up to 1000-1500 MPa, being similar to the results obtained with the GDS EoS at higher pressures. For higher temperatures, all the equations predict similar density values up to 500 MPa (with the exception of DH), whereas at higher pressures the values predicted by means of the Tammann-Tait equation are higher than those obtained using the other four EoSs. In this temperature range, DH and ZW EoSs give rise to the lowest density values. Intermediate values between those obtained with the Tammann-Tait equation and those predicted by the ZW equation were found with the PLDS and GDS EoS (eqs 6 and 9). In general, similar behavior can be observed for the densities of the other oils except for PAO6 and the gear oil (Figures. S2 to S7 of the supplementary information). In general, GDS EoS seems to reproduce more adequately the pressure trend of the volumetric properties. It can be observed that DH and ZW equations rapidly approaches to an asymptotic behavior whereas the Tammann-Tait equation predicts a larger compressible behavior. In the literature[40, 47] it can be found experimental data for glycerol, a silicone oil and a heavy naphthenic mineral oil, among other liquids, indicating larger compressibility at high pressures compared to those predicted with DH equation. As indicated by Venner and Bos,[6] this larger compressibility can be expected to have a significant effect in the central region of the EHL contact.

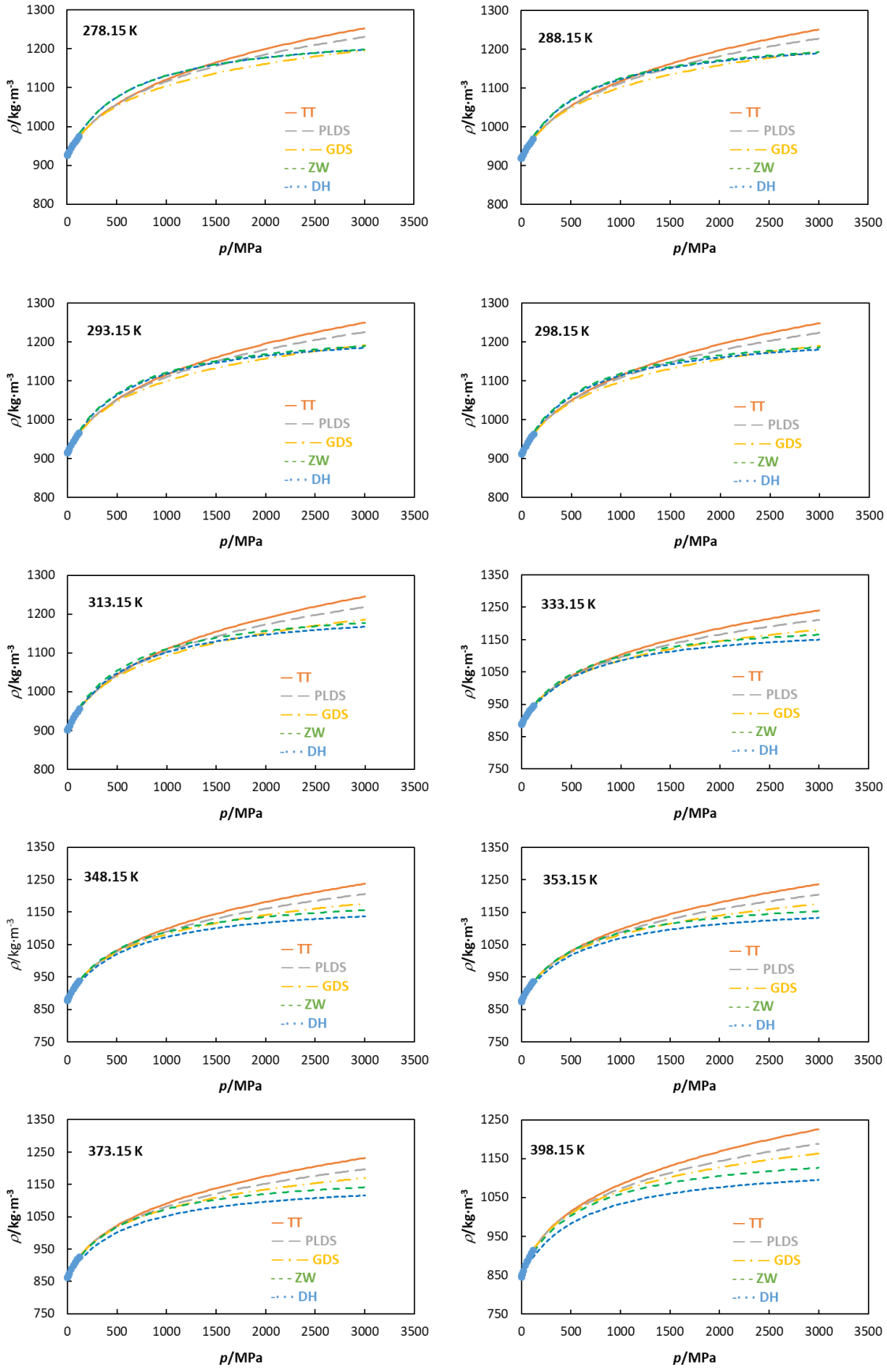

Figure 6. Density of G-V at the different experimental temperatures as a function of pressure according to the EoS: Tammann-Tait (eq 3), PLDS (eq 6), GDS (eq 9), DH (eq 11) and ZW (eq 12).

3.3. Derived Properties. From the three correlation equations (eqs 3, 6 and 9) as well as the predictive equations (eqs 11 and 12) we have estimated the isobaric thermal expansion coefficients, α_p, and the isothermal compressibilities, κ_T, for the base and the formulated oils, using their definitions:

$$\alpha_P = -\frac{1}{\rho}\left(\frac{\partial \rho}{\partial T}\right)_p = \frac{1}{V}\left(\frac{\partial V}{\partial T}\right)_p \quad (14)$$

$$\kappa_T = \frac{1}{\rho}\left(\frac{\partial \rho}{\partial p}\right)_T = -\frac{1}{V}\left(\frac{\partial V}{\partial p}\right)_T \quad (15)$$

The values obtained with the Tammann-Tait correlation (eq 3), PLDS EoS and GDS EoS are reported for the base and formulated oils studied in Tables S4-S9. With the Tammann-Tait correlation, the uncertainty of the α_p values was estimated to be 4%.[40] In the most of the experimental *p-T* conditions PAO6 is the most expandable oil, except for pressures higher than 60 MPa for which it is G-V. Thus, the trend found for this property at low pressures is PAO6 > gear oil ≈ G-III > G-V > motor oil > G-I, and at high pressures G-V > PAO6 > gear oil > G-III > motor oil > G-I.

In the experimental *p-T* range, for all the lubricants, AADs are lower than 2.1% and 2.0% between the α_p values obtained with Tammann-Tait equation and PLDS behavior. The α_p isotherms present crossing points in the experimental range (and GDS, respectively. The α_p values obtained with the three correlations present a complex (Figure S8). Thus α_p decreases always with the pressure but depending of the pressure this property can increase or decrease with the temperature. This behavior was found previously for different compounds.[13, 40, 48, 49] We have calculated α_p also with the predictive DH and ZW EoS. In this case the AADs with the values obtained from Tammann-Tait equation range from 17 to 19% and from 10 to 12%, respectively. We must point out that the predicted α_p values provided by the DH equation are independent on pressure whereas the ZW predictions depend on both pressure and temperature

but are independent of the fluid. Thus, whereas the three correlation equations provide consistent α_p values, both predictive methods are unable to predict satisfactory values due to their simplicity. Larsson *et al.*[50] indicate that α_p influences not only the pressure distribution in EHL but also the energy dissipation due to compression. The thermal expansion is especially important for the performance of hydrodynamic parallel surface thrust bearings because it is the origin of the called thermal wedge.[50] The density- temperature behavior of the lubricants is also an important factor controlling the EHL film thickness.[51]

At low pressures the following sequence was found for isothermal compressibility PAO6 > G-III > gear oil > motor oil > G-I > G-V. Compressibilities of motor base oil, G-I and G-V are quite similar. This is the same trend as for isentropic conditions at 0.1 MPa. At high pressures the following sequence is accomplished: G-V > motor oil > G-I. Thus, as above indicated, PAO6 is the most compressible of the six oils studied in most of the *p*-*T* conditions. As we have pointed out, lubricants with high compressibility give rise to a thinner central oil film than a stiffer lubricant for the same inlet oil film thickness.[8]

The estimated uncertainty for isothermal compressibilities, κ_T in the correlation conditions range using the Tammann-Tait equation is 1%.[52] We have found excellent agreement between the compressibility results of the Tammann-Tait equation and those values obtained with PLDS and GDS EoS. Thus, for all the lubricants AADs are lower than 0.25% and 0.40% for PLDS and GDS, respectively. The AAD% between the κ_T values obtained by the Tammann-Tait correlation in the experimental *p,T* range and those obtained from the predictive equations of DH and ZW EoSs range from 13 to 17% and from 11 to 15% respectively. In Figure 7 it can be seen, how similar are the results obtained at 353.15 K from the three correlation EoS up to 120 MPa. This figure also shows the discrepancy among the experimental values (TT equation) and those predicted using and ZW EoSs.

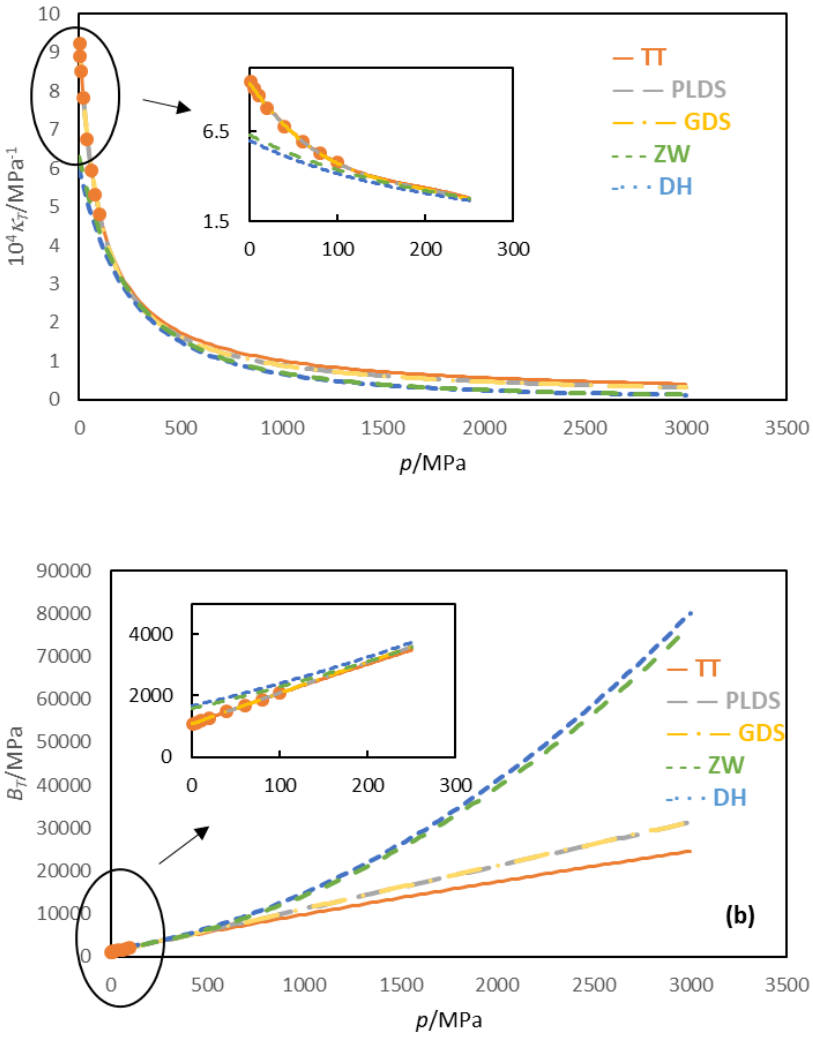

Figure 7. (a) Isothermal compressibility values and (b) its inverse, the bulk modulus, of PAO6 at 353.15 K, extrapolated up to 3000 MPa. Lines represent the prediction and correlation with the EoS: Tammann-Tait, DH , ZW, Grzybowski *et al.* (PLDS and GDS). (●) calculated with eq 3

As for densities, we have also estimated the isothermal compressibilities up to 3000 MPa with the five EoSs. As can be observed in Figure–7 significant differences were found among the extrapolated results obtained with the Tammann-Tait equation and those predicted by DH and ZW being the results provided by these two last equations very similar, with an AAD of 3.2%. DH (eq 11) and ZW (eq 12) are not able to predict compressibilities even at low

pressures. For the six oils studies up to 3000 MPa (see also Figures. 2 to 7 in the supplementary information) AADs higher than 36% were found between the values corresponding to the Tammann-Tait equation and those predicted by eqs 11 and 12.

4. Conclusions

New experimental density data as a function of pressure and temperature were correlated with Tammann-Tait (TT), Power-Law Density Scaling (PLDS) and General Density Scaling (GDS) EoSs, being the average absolute deviations between experimental and correlated data lower than 0.03%. The Dowson-Higginson (DH), Zhu and Wen (ZH) and Jacobson-Vinet (JV) EoSs, currently used in numerical simulations of the isothermal EHL lubrication regime predict these densities with high average deviations: 0.50%, 0.34% and 0.74% respectively. The sequence we have found at low pressures is the same for isothermal and for isentropic compressibility: PAO6>G-III>gear oil>motor oil>G-I> G-V. At high pressures G-V presents higher compressibilities than motor oil and G-I. PAO6 is also the most expansible oil in most experimental *p-T* conditions. Excellent agreement has been found between the isothermal compressibility, and isobaric thermal expansivity, determined from PLDS and GDS EoSs and those values determined from Tammann-Tait equation. Thus, average absolute deviations lower than 0.40% and 2.1% have been found for κ_T and α_P, respectively. Nevertheless, the α_P and κ_T values obtained with DH and ZW EoSs present average deviations with those values obtained with the Tammann-Tait correlation ranging from 17 to 19% and from 10 to 12% for α_P and for κ_T from 13 to 17% and from 11 to 15%. Due to the fact that the maximum contact pressure in EHL lubrication can reach values up to 3000 MPa, much higher than the pressure interval achieved with oscillating tube densimeters, we have also analysed the extrapolation ability of five of the above equations. We can conclude that both DH and ZH models underestimates the compressibility at high pressures and temperatures higher than 313 K because of the asymptotic

limited density value, whereas GDS EoS seems to provide better extrapolations. That means that DH and ZH equations are unable to perform a satisfactory prediction due to their simplicity. This paper shows the importance to properly take into account the oil compressibility on EHL simulations at very high pressures.

Supporting information

The Supporting Information is available free of charge on the ACS Publications website.

Tables S1, S2 and S4 summarize the experimental data; Tables S3, S5 and S6 report the parameters of the different correlation equations; Tables S7-S12 summarize the values of the thermal expansion coefficients and isothermal compressibilities provided by TT, PLDS and GDS EoS; Figures S2-S7 show different volumetric properties together with the results of the different EoS used; Figure S8 represents the pressure and temperature dependence of the thermal expansion coefficients obtained from the TT correlation equation.

Acknowledgments

We are grateful to Profs. N. Ohno and T. Mawatari (Saga University, Japan) to provide us with unpublished values of the SN100 traction oil. We would like to thank Dr. L. Fernández Ruiz-Morón (REPSOL, Madrid) for providing our laboratory with the lubricant samples. Authors wish express their gratitude to Dr. T. Regueira for her assistance with the predictive equations. This work was supported by Spanish Ministry of Economy and Competitiveness and the UE FEDER programme through ENE2014-55489-C2-1-R project. Moreover, this work was funded by the Xunta de Galicia (AGRUP2015/11 and GRC ED431C 2016/001).

References

1. Vergne, P. *Static and dynamic compressibility of lubricants under high pressure*. Elsevier: Amsterdam-London-New York-Tokio, 1995.
2. Neale, M. J. *The Tribology Handbook*. Second ed.; Butterworth-Heinemann: Oxford, 1995.
3. Regueira, T.; Lugo, L.; Fandiño, O.; López, E. R.; Fernández, J. Compressibilities and viscosities of reference and vegetable oils for their use as hydraulic fluids and lubricants. *Green Chem.* **2011,** *13*, 1293-1302.
4. Stachowiak, G. W.; Batchelor, A. W. *Engineering tribology*. 3rd ed.; Elsevier Butterworth-Heinemann: Amsterdam, 2005.
5. Errichello, R. Elastohydrodynamic Lubrication (EHL): A Review. *Gear Technology* **2015,** July 2015, 60-62.
6. Venner, C. H.; Bos, J. Effects of lubricant compressibility on the film thickness in EHL line and circular contacts. *Wear* **1994,** *173*, 151-165.
7. Höglund, E. Influence of lubricant properties on elastohydrodynamic lubrication. *Wear* **1999,** 232, 176-184.
8. Jacobson, B. O. *Rheology and Elastohydrodynamic Lubrication*. 1st Edition; Elsevier, 1991.
9. Hamrock, B. J.; Pan, P.; Lee, R. T. Pressure spikes in elastohydrodynamically lubricated conjunctions. *ASME Journal of Tribology* **1988,** *110*, 279-284.
10. Mia, S.; Ohno, N. Prediction of pressure–viscosity coefficient of lubricating oils based on sound velocity. *Lubr. Sci.* **2009,** *21*, 343-354.
11. Mia, S. Prediction of Tribological and Rheological Properties of Lubricating Oils by Sound Velocity. PhD Thesis, Saga University, 2010.
12. Grzybowski, A.; Grzybowska, K.; Paluch, M.; Swiety, A.; Koperwa, K. Density scaling in viscous systems near the glass transition. *Phys. Rev. E* **2011,** *83*, 041505.
13. Chorążewski, M.; Grzybowski, A.; Paluch, M. Isobaric Thermal Expansion of Compressed 1,4-Dichlorobutane and 1-Bromo-4-chlorobutane: Transitiometric Results and a Novel Application of the General Density Scaling-Based Equation of State. *Ind. Eng. Chem. Res.* **2015,** *54*, 6400-6407.
14. Grzybowski, A.; Koperwas, K.; Paluch, M. Equation of state in the generalized density scaling regime studied from ambient to ultra-high pressure conditions. *J. Chem. Phys.* **2014,** *140*, 044502.

15. Dowson, D.; Higginson, G. R. *Elastohydrodynamic lubrication, The Fundamental of Roller and Gear Lubrication*. Pergamon: Oxford, 1966.

16. Dowson, D.; Higginson, G. R.; Whitaker, A. V. Elasto-hydrodynamic lubrication: a survey of isothermal solutions. *J. Mech. Eng. Sci.* **1962,** *4*, 121-126.

17. Zhu, D.; Wen, S. Z. A full numerical-solution for the thermoelastohydrodynamic problem in elliptical contacts *J. Tribol.* **1984,** *106*, 246-254.

18. Jacobson, B. O.; Vinet, P. A model for the influence of pressure on the bulk modulus and the influence of temperature on the solidification pressure for liquid lubricants. *J. Tribol.* **1987,** *109*, 709-714.

19. Novotny-Farkas, F.; Böhme, W.; Stabinger, H.; Belitsch, W. The Stabinger Viscometer a new and unique instrument for oil service laboratories. *Anton Paar* World Tribology Congress II, 2001.

20. Paredes, X.; Fandiño, O.; Comuñas, M. J. P.; Pensado, A. S.; Fernández, J. Study of the effects of pressure on the viscosity and density of diisodecyl phthalate. *J. Chem. Thermodyn.* **2009,** *41*, 1007-1015.

21. Gaciño, F. M.; Regueira, T.; Lugo, L.; Comuñas, M. J. P.; Fernández, J. Influence of Molecular Structure on Densities and Viscosities of Several Ionic Liquids. *J. Chem. Eng. Data* **2011,** *56*, 4984-4999.

22. Carvalho, P. J.; Regueira, T.; Santos, L. M. N. B. F.; Fernandez, J.; Coutinho, J. A. P. Effect of water on the viscosities and densities of 1-butyl-3-methylimidazolium dicyanamide and 1-butyl-3-methylimidazolium tricyanomethane at atmospheric pressure. *J. Chem. Eng. Data* **2009,** *55*, 645-652.

23. Segovia, J. J.; Fandiño, O.; López, E. R.; Lugo, L.; Martín, M. C.; Fernández, J. Automated densimetric system: Measurements and uncertainties for compressed fluids. *J. Chem. Thermodyn.* **2009,** *41*, 632-638.

24. Regueira, T.; Lugo, L.; Fernández, J. High pressure volumetric properties of 1-ethyl-3-methylimidazolium ethylsulfate and 1-(2-methoxyethyl)-1-methyl-pyrrolidinium bis(trifluoromethylsulfonyl)imide. *J. Chem. Thermodyn.* **2012,** *48*, 213-220.

25. Regueira, T.; Lugo, L.; Fernández, J. Influence of the pressure, temperature, cation and anion on the volumetric properties of ionic liquids: New experimental values for two salts. *J. Chem. Thermodyn.* **2013,** *58*, 440-448.

26. Laesecke, A.; Outcalt, S. L.; Brumback, K. J. Density and speed of sound measurements of methyl- and propylcyclohexane. *Energy & Fuels* **2008,** *22*, 2629-2636.

27. Outcalt, S.; Laesecke, A.; Freund, M. B. Density and speed of sound measurements of jet A and S-8 aviation turbine fuels. *Energy & Fuels* **2009,** *23*, 1626-1633.

28. Saryazdi, F.; Motahhari, H.; Schoeggl, F. F.; Taylor, S. D.; Yarranton, H. W. Density of hydrocarbon mixtures and bitumen diluted with solvents and dissolved gases. *Energy & Fuels* **2013,** *27*, 3666-3678.

29. Wagner, W.; Pruss, A. The IAPWS Formulation 1995 for the Thermodynamic Properties of Ordinary Water Substance for General and Scientific Use. *J. Phys. Chem. Ref. Data* **2002,** *31*, 387-535.

30. Cibulka, I. Saturated liquid densities of 1-alkanols from C_1 to C_{10} and n-alkanes from C_5 to C_{16}: a critical evaluation of experimental data. *Fluid Phase Equilibr.* **1993,** *89*, 1-18.

31. Cibulka, I.; Hnědkovský, L. Liquid Densities at Elevated Pressures of n-Alkanes from C_5 to C_{16}: A Critical Evaluation of Experimental Data. *J. Chem. Eng. Data* **1996,** *41*, 657-668.

32. Comuñas, M. J. P.; Bazile, J.-P.; Baylaucq, A.; Boned, C. Density of diethyl adipate using a new vibrating tube densimeter from (293.15 to 403.15) K and up to 140 MPa. Calibration and measurements. *J. Chem. Eng. Data* **2008,** *53*, 986-994.

33. Mia, S.; Ohno, N. Relation between low temperature fluidity and sound velocity of lubricating oil. *Tribol. Int.* **2010,** *43*, 1043-1047.

34. Comuñas, M. J. P.; Reghem, P.; Baylaucq, A.; Boned, C.; Fernández, J. High-Pressure Volumetric Properties of Three Monoethylene Glycol Alkyl Ethers. *J. Chem. Eng. Data* **2004,** *49*, 1344-1349.

35. Debenedetti, P. G.; Stillinger, F. H. Supercooled liquids and the glass transition. *Nature* **2001,** *410*.

36. Noday, D. A.; Steif, P. S.; Rabin, Y. Viscosity of cryoprotective agents near glass transition: a new device, technique, and data on DMSO, DP6, and VS55. *Exp. Mech.* **2009,** *49*, 663-672.

37. Otero, I.; López, E. R.; Reichelt, M.; Villanueva, M.; Salgado, J.; Fernández, J. Ionic Liquids Based on Phosphonium Cations As Neat Lubricants or Lubricant Additives for a Steel/Steel Contact. *ACS Appl. Mater. Interfaces* **2014,** *6*, 13115−13128.

38. Pensado, A. S.; Padua, A. A. H.; Comuñas, M. J. P.; Fernández, J. Relationship between Viscosity Coefficients and Volumetric Properties Using a Scaling Concept for Molecular and Ionic Liquids. *J. Phys. Chem. B* **2008,** *112*, 5563-5574.

39. Bair, S. S.; Andersson, O.; Qureshi, F. S.; Schirru, M. M. New EHL Modeling Data for the Reference Liquids Squalane and Squalane Plus Polyisoprene. *Tribol. Trans.* **2017,** in press.

40. Regueira, T.; Lugo, L.; Fernández, J. Compressibilities and Viscosities of Reference, Vegetable, and Synthetic Gear Lubricants. *Ind. Eng. Chem. Res.* **2014,** *53*, 4499−4510.

41. Hamrock, B. J.; Schmid, S. R.; Jacobson, B. O. *Fundamentals of fluid film lubrication*. 2nd ed.; Marcel Dekker, cop.: New York, 2004.

42. Martins, R.; Seabra, J.; Brito, A.; Seyfert, C.; Luther, R.; Igartua, A. Friction coefficient in FZG gears lubricated with industrial gear oils: Biodegradable ester vs. mineral oil. *Tribol. Int.* **2006,** *39*, 512-521.

43. Errichello, R. Selecting Oils with High Pressure-Viscosity Coefficient - Increase Bearing Life by More Than Four Times. *Machinery Lubrication* **2004,** March.

44. Ohno, N.; Rahman, M. Z.; Kakuda, K. Bulk Modulus of Lubricating Oils as Predominant Factor Affecting Tractional Behavior in High-Pressure Elastohydrodynamic Contacts. *Tribol. Trans.* **2005,** *48*, 165-170.

45. Ohno, N.; Mawatari, T. Personal Communication. **2017**.

46. Bair, S. S. *High-pressure rheology for quantitative elastohydrodynamics*. 1st ed.; Elsevier: Amsterdam, 2007.

47. Habchi, W.; Bair, S. Quantitative compressibility effects in thermal elastohydrodynamic circular contacts. *J. Tribol.* **2013,** *135*, 011502-1-011502-10.

48. Gaciño, F. M.; Regueira, T.; Bolotov, A. V.; Sharipov, A.; Lugo, L.; Comuñas, M. J. P.; Fernández, J. Volumetric behaviour of six ionic liquids from T = (278 to 398) K and up to 120 MPa. *J. Chem. Thermodyn.* **2016,** *93*, 24-33.

49. Chorążewski, M.; Grzybowski, A.; Paluch, M. The complex, non-monotonic thermal response of the volumetric space of simple liquids. *Phys. Chem. Chem. Phys.* **2014,** *16*, 19900-19908.

50. Larsson, R.; Larsson, P. O.; Eriksson, E.; Sjöberg, M.; Höglund, E. Lubricant properties for input to hydrodynamic and elastohydrodynamic lubrication analyses. *Proc. Inst. Mech. Eng. Part J-J. Eng. Tribol.* **2000,** *214*, 17-27.

51. Kaneta, M.; Yang, P.; Krupka, I.; Hartl, M. Fundamentals of thermal elastohydrodynamic lubrication in Si_3N_4 and steel circular contacts. *Proc. Inst. Mech. Eng. Part J-J. Eng. Tribol.* **2015,** *229*, 929-939.

52. Comuñas, M. J. P.; Gaciño, F. M.; Cabaleiro, D.; Lugo, L.; Fernández, J. Krytox GPL102 Oil as Reference Fluid for High Viscosities: High Pressure Volumetric Properties, Heat Capacities, and Thermal Conductivities. *J. Chem. Eng. Data* **2015,** *60*, 3660−3669.

Table of Content Graphic